Submicron cubic boron nitride as hard as diamond

Guoduan Liu,[1] Zili Kou,[1,a)] Xiaozhi Yan,[1,2,a)] Li Lei,[1] Fang Peng,[1] Qiming Wang,[1] Kaixue Wang,[1] Pei Wang,[1] Liang Li,[1] Yong Li,[1] Wentao Li,[1,2] Yonghua Wang,[1] Yan Bi,[3] Yang Leng,[4] and Duanwei He[1,3]

[1]*Institute of Atomic and Molecular Physics, Sichuan University, Chengdu 610065, People's Republic of China*
[2]*Center for High Pressure Science and Technology Advanced Research (HPSTAR), Shanghai 201203, People's Republic of China*
[3]*Institute of Fluid Physics and National Key Laboratory of Shockwave and Detonation Physic, China Academy of Engineering Physics, Mianyang 621900, People's Republic of China*
[4]*Department of Mechanical Engineering, Hong Kong University of Science and Technology, Kowloon, Hong Kong, People's Republic of China*

Here, we report the sintering of aggregated submicron cubic boron nitride (sm-cBN) at a pressure of 8 GPa. The sintered cBN compacts exhibit hardness values comparable to that of single crystal diamond, fracture toughness about 5-fold that of cBN single crystal, in combination with a high oxidization temperature. Thus, another way has been demonstrated to improve the mechanical properties of cBN besides reducing the grain size to nano scale. In contrast to other ultrahard compacts with similar hardness, the sm-cBN aggregates are better placed for potential industrial application, as their relative low pressure manufacturing perhaps be easier and cheaper. © 2015 AIP Publishing LLC. [http://dx.doi.org/10.1063/1.4915253]

Synthetic cubic boron nitride (cBN) and diamond are the two artificial super-hard materials that have been most widely used in industry for over half a century.[1,2] cBN possesses high thermal and chemical stability superior to those of diamond,[3] and it is the best-known material for cutting ferrous and carbide-forming hard substances where diamond completely fails.[4] However, the hardness of cBN is much lower than that of diamond (the single crystal cBN has Vickers hardness (Hv) of about 50 GPa, while for single crystal diamond this value is about 60–120 GPa; corresponding values are lower for commercially used polycrystalline cBN and diamond (PCD)).[5–7] For decades, various ways have been designed to increase the hardness of polycrystalline cBN, and the synthesis of nanocrystalline cBN seems to be the most effective way.[8–10]

In polycrystalline materials, grain boundaries can effectively hinder the movements of dislocations and improve the strength, thereby enhance the hardness of polycrystalline aggregates.[11] As the total area of grain boundaries increase with the decreasing crystalline size, nanocrystalline aggregates should be noticeably harder as compared to its microcrystalline counterparts.[12,13] This increase in hardness with decreasing crystal size is known as the Hall-Petch effect.[14,15] Following this route, nanocrystalline cBNs have been synthesized at high pressure and temperature and demonstrate some noticeable improvement of hardness.[8,9,16] But the synthetical pressure for those nano-cBNs (∼20 GPa) is much higher than that for commercial cBN (∼5.5 GPa), while other phases instead of cubic phase of boron nitride are used as starting materials. The application of nano-cBN is therefore limited.

Is nano-cBN synthesized at such a high pressure from precursor the only solution for remarkable hardness improvement of cBN? Defects (e.g., twins and stacking faults) in crystallines and the interfacial bonding between grains also have an important influence on the strength of materials just like grain boundaries.[11,12,17] So, theoretically speaking, the hardness of cBN can also be increased by introducing defects and well bonded interface. In this study, we present the sintering of super-hard submicron cubic boron nitride (sm-cBN) compacts starting from pre-synthesized cBN powder at a mild pressure of ∼8 GPa and high temperatures of 1800–2400 K. No binders of other materials are used as they may reduce the strength of interfaces and lower the hardness of the products.[12] Because of the high hardness of each cBN crystalline, large local stress may arise when grains were compacted under high pressure and defects may be introduced by this local stress.

Pure cubic BN powder with diameter about 0.2–0.5 μm was used as the starting material after vacuum heat-treatment at 1500 K. High pressure and high-temperature (HPHT) experiments were carried out with a DS 6×14 MN cubic press. The cell temperature was measured directly using a W-Re thermocouple, and the pressure was estimated from previously obtained calibration curve. Samples were gradually compressed to 8 GPa at ambient temperature, and then the temperature was stepwise increased with a heating rate of about 100 K min^{-1} to the desired value. The duration of heating was 15 min. The samples were quenched at a rate of about 200 K min^{-1} and then slowly decompressed.

The phase composition of the sintered samples was investigated by the X-ray diffraction (XRD) analysis with CuKα radiation (DX-2500, Dandong, China). Microstructures of sintered samples were characterized by Transmission Electron Microscopy (TEM) (Tecnai G2 F20 S-TWIN) with an accelerating voltage of 200 kV. Vickers hardness of the polished samples was tested by a Vickers hardness tester (FV-700B, Future-Tech, Japan). Ultrasonic experiment is measured by JDUT-2 ultrasonic instrument (LECROY, WR6050A, USA).

a)Authors to whom correspondence should be addressed. Electronic addresses: kouzili@scu.edu.cn and yanxz@hpstar.ac.cn
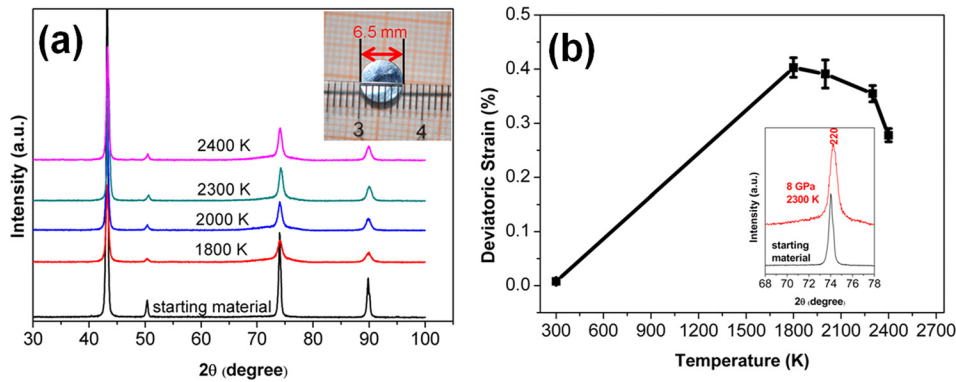
FIG. 1. X-ray diffraction analysis and photograph of sm-cBN samples. (a) XRD patterns of starting material and samples sintered at 8 GPa and various temperatures. Inset: optical microscopic image of a sm-cBN sample sintered at 8 GPa and 2300 K (about 6.5 mm in diameter and 4 mm thick). (b) Deviatoric strain of sm-cBN aggregates versus sintering temperature. Inset: (2 2 0) peaks in XRD patterns of starting material and sample sintered at 8 GPa and 2300 K.

Studies on oxidation resistance were performed in air using the NETZSCH STA 449C with a heating rate of 10 K min^{-1} from 300 K to 1750 K. Cutting tests were conducted on a numerically controlled lathe (SK50P/750, Baoji, China). Tool holders were CRSNR2525M09. The tool wear was gauged by a stereomicroscope (XTL-3400, Shanghai, China). No lubricant or coolant was used during turning.

The well sintered samples are cylinder-shaped chunks with a diameter of about 6.5 mm and thickness of about 4 mm after polishing (inset of Figure 1(a)). Figure 1(a) shows XRD patterns of the starting cBN and samples sintered at different temperatures. There are no other XRD peaks existing in these patterns besides peaks which belong to cBN. It means that no XRD detectable impurities were introduced. This may be a result of that no sintering aids were used in the present study and mixing process was avoided, in which impurities are apt to be introduced. Another feature of the XRD patterns of samples treated at HPHT is that the diffraction peaks are broadened compared to starting material (inset of Figure 1(b)). The deviatoric strains of samples have been analyzed from the XRD line broadening using the following relation:

$$\text{FWHM}^2 \cos^2\theta = \left(\frac{\lambda}{d}\right)^2 + \sigma^2 \sin^2\theta \qquad (1)$$

where FWHM is the full-width at half-maximum of the diffraction profile on 2θ-scale. The symbols d, λ, and σ denote the grain size, X-ray wavelength, and deviatoric strain, respectively.

The results (the data at 300 K in Figure 1(b)) show that the deviatoric strain of starting material is nearly zero, while the values for cBNs sintered at HPHT are significantly increased. As the deviatoric strain of crystallines is primarily resulted from defects in material,[18] the obtained deviatoric strain values indicate that the starting material is almost defect free while defects were introduced after HPHT treatment, and the defect concentration in samples decreases with increasing sintering temperature.

Typical TEM and high-resolution TEM (HRTEM) images of the sample synthesized at 8 GPa and 2300 K are shown in Figs. 2(a)–2(c). It can be seen that the grain size is mainly about 0.2–0.5 μm (Figure 2(a)). Densely spaced twin boundaries and stacking faults are seen in grains (Figures 2(b) and 2(c)), and the length between twin boundaries or stacking faults are predominantly in nanoscale. In other words, perfect crystals of cBN are divided into nanoscale dimensions along directions perpendicular to the twin boundaries or stacking faults. Similar features have also been found in the recent reported cBN sample synthesized from specially prepared boron nitride precursor possessing onion-like nested structures.[10] The defects (such as stacking faults) lead to deviatoric strain in the sample and give rise to the broadening of the XRD peaks, consisting with the XRD observation.

Ultrasonic measurements have been performed to give the modulus values of sm-cBN using a pulse-echo method.[19] By dividing the round-trip distance by the pulse transit time (t), the wave velocity has been calculated. The values of Young's modulus (E), bulk modulus (B), shear modulus (G), and Poisson's ratio (ν) have been calculated from the densities of the sintered samples measured with Archimedes method, making use of the longitudinal and transverse velocities of the acoustic waves. Table I lists the values of ρ, E, G, and B for the sample sintered at HPHT, while the corresponding theoretic values as well as the reported bulk modulus of other super hard materials are also listed.[8,13,20,22,24] For the sample sintered at 8 GPa and 2300 K, the density reaches 3.48 g/cm^3, almost the same with the theoretical value (3.49 g/cm^3). Also, the modulus values (Young's modulus ($\sim$901 GPa), bulk modulus ($\sim$384 GPa), and shear modulus ($\sim$406 GPa)) are close to the theoretical values of cBN.
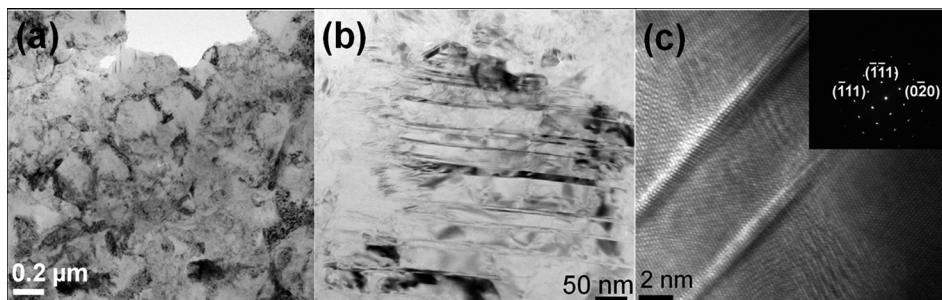

FIG. 2. TEM characterization of the sample sintered at 8 GPa and 2300 K. (a) Low-magnification TEM image of the sm-cBN sample. (b) TEM image of substructure in a submicron grain. (c) HRTEM image of a sm-cBN. Inset: the corresponding selected area electron diffraction pattern.

TABLE I. Typical mechanical properties of sm-cBN and its comparison with other super hard materials.

Samples	H_v (GPa)	ρ (g/cm^3)	E (GPa)	B (GPa)	G (GPa)
sm-cBN	75	3.48	901	384	406
Diamond composite[a,b]	51	3.47	446	183	204
cBN composite[c,d]	36	4.28	587	254	284
Nano-cBN[e,f]	…	…	875	375	…
Theoretical[g]	…	3.49	909	400	405

[a,b]Experimental data from Refs. 21 and 22.
[c,d]Experimental data from Refs. 23 and 24.
[e,f]Experimental data from Refs. 8 and 13.
[g]Experimental data from Ref. 20.

Vickers Hardness of the polished cBN samples was measured using a standard square-pyramidal diamond indenter with a holding time of 15 s. Figure 3(a) shows the load dependence of the Vickers hardness for the specimen sintered at 8 GPa and 2300 K. The value of Vickers hardness was 112 ($\pm$3) GPa at the load of 2.94 N, similar to the hardness of nanotwinned cBN (108 GPa) under the same loading, which has been claimed to be the highest hardness reported so far for polycrystalline cBN.[10] However, it has been suggested that much higher loads are required for saturation of population growth of microcracks in a brittle material to report a correct hardness value.[25–27] Thus, we continue to test the hardness with larger loading force up to 98 N. By increasing the loading force to 29.4 N, the hardness reaches the asymptotic value of 75 ($\pm$3) GPa, and then almost remain unchanged at loads above 29.4 N. This hardness value is much higher than that of single crystal cBN ($\sim$50 GPa) and comparable to that of single crystal diamond (60–120 GPa).[10,28,29] Table I lists the values of H_v for the sintered sample and the corresponding values of diamond composite and cBN composite from literatures.[21,23] It could be seen that the hardness of sm-cBN is much higher than that of diamond composite and cBN composite.

The fracture toughness of the sintered samples have been determined by the equation of $K_{IC} = \xi (E/H_V)^{1/2} (P/c^{3/2})$ (MPa m$^{1/2}$),[30,31] where ξ is a calibration constant of 0.0166 ($\pm$0.004), E is the Young's modulus (GPa), P is the loading force (N), and c is the length of the crack. The resulting K_{IC} of sample sintered at 8 GPa and 2300 K reaches 13.2 MPa m$^{1/2}$,

which is about 3-fold that of single crystal diamond (3.4–5 MPa m$^{1/2}$)[5] and almost 5-fold that of single crystal cBN (2.8 MPa m$^{1/2}$).[8]

The extraordinary hardness and fracture toughness reported here may be attributed to three factors: First, the XRD linewidth analysis (Figure 1(b)) and TEM images (Figures 2(b) and 2(c)) indicate that defects (mainly including stacking faults and twins) were introduced in the sintering process. The defects in crystallines act as obstacles for dislocation glide during deformation,[11] and the strength of cBN is therefore improved; thus, this way has also been demonstrated to improve the mechanical properties of cBN besides of reducing the grain size to nano scale; second, the sintered sample was highly condensed and well sintered, indicated by the density and modulus values of sm-cBN which are very close to theoretic values; third, the strength of cBN aggregate with submicron grain could be enhanced compared with conventional cBN with micron grain size due to the Hall-Petch effect.[14,15]

The thermal stability of the cBN sample sintered at 8 GPa and 2300 K has been investigated by thermoanalytical (TG) characterization. Figure 3(b) shows a onset oxidation temperature of 1525 K in air for the as prepared sm-cBN, which is higher than those of single crystal cBN ($\sim$1376 K) (Ref. 10) and nanograined cBN ($\sim$1460 K) (inset of Figure 3(b)).[8]

Cutting tests have also been conducted on the sintered samples and commercial cBN. The samples are used for the high-speed cutting of hardened steel (hardness of the hardened steel: HRc = 62, cutting speed: 120 m/min, feed: 0.15 mm/rev, and depth of cut: 0.1 mm). Tool wear was represented by the width of wear on the flank surface (Vb) (inset of Figure 3(c)), and was used to evaluate the wear performance of the sintered samples. Figure 3(c) compares the wear performance of the sample prepared at 8 GPa and 2300 K to the commercial cBN. It could be seen that the wear of sintered sample is more narrow than that of commercial cBN at the same cutting time, indicating a better wear resistance of the sm-cBN.

In summary, it has been shown that defects including stacking faults and twins could be introduced into sm-cBN in the HPHT sintering, and the mechanical properties of the well sintered highly condensed sm-cBN aggregates were
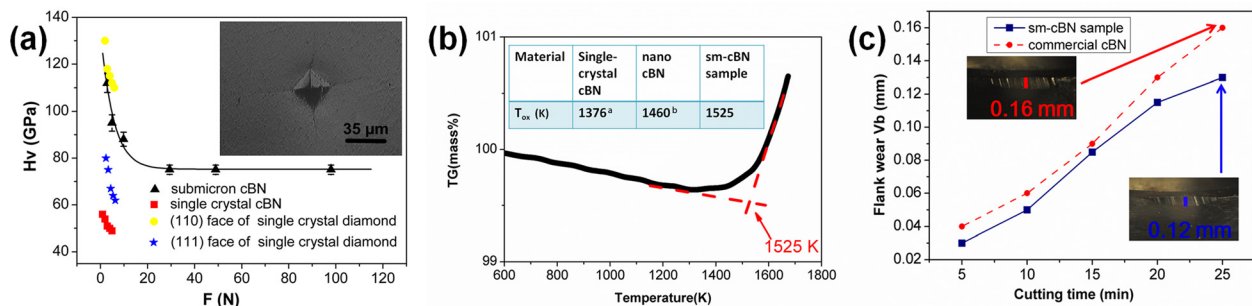

FIG. 3. Properties of a sample sintered at 8 GPa and 2300 K. (a) Vickers hardness as a function of applied load force. Inset: an optical micrograph of the Vickers indentation with cracks produced at a load of 49 N. For single crystal cBN, the value of Vickers hardness is $\sim$50 GPa; for the single crystal diamond, the values of Vickers hardness are $\sim$110 GPa on the {1 1 0} face and $\sim$62 GPa on the {1 1 1} face.[10,13] (b) The thermogravimetric curve for sm-cBN sample. Inset: table showing oxidation temperatures of different cBN samples. ([a]Experimental data from Ref. 10, [b]Experimental data from Ref. 8.). (c) The width of wear on the as prepared sm-cBN sample and commercial cBN as functions of cutting time. Inset: photographs of the sm-cBN samples at a cutting time of 25 min.

improved by these defects. This makes it possible to sinter sm-cBN aggregate with mechanical properties and thermo-stability comparable with or better than those of single cystal diamond at a moderate pressure, and thus open unique opportunities for the industrial applications of this material.

[1]F. P. Bundy, H. T. Hall, R. H. Strong, and R. H. Wentorf, Nature. **176**, 51 (1955).
[2]R. H. Wentorf, J. Chem. Phys. **26**, 956 (1957).
[3]V. L. Solozhenko and V. Z. Turkevich, J. Therm. Anal. **38**, 1181 (1992).
[4]N. Dubrovinskaia, L. Dubrovinsky, W. Crichton, F. Langenhorst, and A. Richter, Appl. Phys. Lett. **87**, 083106 (2005).
[5]N. Dubrovinskaia, S. Dub, and L. Dubrovinsky, Nano Lett. **6**, 824 (2006).
[6]T. Taniguchi, M. Akaishi, and S. Yamaoka, J. Am. Ceram. Soc. **79**, 547 (1996).
[7]T. Taniguchi, M. Akaishi, and S. Yamaoka, J. Mater. Res. **14**, 162 (1999).
[8]V. L. Solozhenko, O. O. Kurakevych, and Y. Le Godec, Adv. Mater. **24**, 1540 (2012).
[9]N. Dubrovinskaia, V. L. Solozhenko, N. Miyajima, V. Dmitriev, O. O. Kurakevych, and L. Dubrovinsky, Appl. Phys. Lett. **90**, 101912 (2007).
[10]Y. J. Tian, B. Xu, D. L. Yu, Y. M. Ma, Y. B. Wang, Y. B. Jiang, W. T. Hu, C. C. Tang, Y. F. Gao, K. Luo *et al.*, Nature **493**, 385 (2013).
[11]S. Karato, *Deformation of Earth Materials: An Introduction to The Rheology of Solid Earth* (Cambridge University Press, New York, 2008), p. 280.
[12]T. Irifune, A. Kurio, S. Sakamoto, T. Inoue, and H. Sumiya, Nature **421**, 599 (2003).
[13]H. Sumiya and T. Irifune, J. Mater. Res. **22**, 2345 (2007).
[14]E. O. Hall, Proc. Phys. Soc. B **64**, 747 (1951).
[15]N. J. Petch, J. Iron Steel Inst., London **174**, 25 (1953).
[16]S. N. Dub and I. A. Petrusha, High Pressure Res. **26**, 71 (2006).
[17]G. D. Zhan, J. D. Kuntz, J. Wan, and A. K. Mukherjee, Nat. Mater. **2**, 38 (2003).
[18]T. Ungár and G. Tichy, Phys. Status Solidi A **171**, 425 (1999).
[19]S. Eros and J. R. Reitz, J. Appl. Phys. **29**, 683 (1958).
[20]M. P. D'Evelyn and T. Taniguchi, Diamond Relat. Mater. **8**, 1522 (1999).
[21]E. A. Ekimov, A. G. Gavriliuk, B. Palosz, S. Gierlotka, P. Dluzewski, E. Tatianin, Yu. Kluev, A. M. Naletov, and A. Presz, Appl. Phys. Lett. **77**, 954 (2000).
[22]H. K. Wang, D. W. He, C. Xu, M. J. Tang, Y. Li, H. N. Dong, C. M. Meng, Z. G. Wang, and W. J. Zhu, J. Appl. Phys. **113**, 043505 (2013).
[23]L. L. Zhang, Z. L. Kou, C. Xu, K. X. Wang, C. L. Liu, B. Hui, and D. W. He, Diamond Relat. Mater. **29**, 84 (2012).
[24]Y. K. Chou and C. J. Evans, Wear **225**, 234 (1999).
[25]N. Dubrovinskaia and L. Dubrovinsky, Nature **502**, E1 (2013).
[26]Y. S. Zhao, J. Qian, L. L. Daemen, C. Pantea, J. Z. Zhang, G. A. Voronin, and T. W. Zerda, Appl. Phys. Lett. **84**, 1356 (2004).
[27]V. Brazhkin, N. Dubrovinskaia, M. Nicol, N. Novikov, R. Riedel, V. Solozhenko, and Y. S. Zhao, Nat. Mater. **3**, 576 (2004).
[28]C. S. Yan, H. K. Mao, W. Li, J. Qian, Y. Zhao, and R. J. Hemley, Phys. Status Solidi A **201**, 25 (2004).
[29]Q. Huang, D. L. Yu, B. Xu, W. T. Hu, Y. M. Ma, Y. B. Wang, Z. S. Zhao, B. Wen, J. L. He, Y. J. Tian *et al.*, Nature **510**, 250 (2014).
[30]G. R. Anstis, P. Chantikul, B. R. Lawn, and D. B. Marshall, J. Am. Chem. Soc. **64**, 533 (1981).
[31]A. G. Evans and E. A. Charles, J. Am. Ceram. Soc. **59**, 371 (1976).